

THIRTEENTH EUROPEAN ROTORCRAFT FORUM

11.3

Paper No. 19

DYNAMIC BEHAVIOUR OF A COMPOSITE
TAIL UNIT FOR EH101

Bruno Maino - Giorgio Vignati

AGUSTA - ITALIA

September 8 - 11, 1987

ARLES, FRANCE

**DYNAMIC BEHAVIOUR OF A COMPOSITE
TAIL UNIT FOR BH101**

Bruno Maino - Giorgio Vignati
Acoustics & Vibration Engineers

Costr. Aeronautiche G. Agusta, Italia

Abstract

In order to verify the reliability of the design criteria for composites for BH101 tail unit and to define a calculation tool, it was decided to build a scaled down model tail unit. The scaled down model has been constructed strictly respecting the manufacturing details of the full scale item.

The scaled down model has been subjected to a vibration test to determine its dynamic behaviour, to verify its modal characteristics and the importance of these in a structure realized completely with composite material.

Different methods of excitation have been employed and their efficiency is discussed.

1.0 Introduction

Composite materials are being employed more and more in the aerospace industry and their use in a large size modern high technology helicopter like the BH101 is quite logical.

The tail unit is one of the sub-structures designed in composite material for the BH101. In order to get a better insight into and develop the technology of "designing" in composites it was decided to build a scaled down model of the original composite tail unit but similar to it in all its manufacturing details and subject it to various mechanical tests. As dynamic behaviour is one of the most important characteristics to be considered the model has been subjected to a vibration test to determine its modal characteristics. A test programme involving different methods of excitation and analysis was followed.

2.0 Test Programme

2.1 The specimen

The specimen used for the vibration tests was a scaled model (3/4) of the original composite tail unit. A picture of the model tail unit is shown in figure 1.

The specimen consisted of unidirectional carbon fibres and carbon fabric arranged opportunely.

2.2 Instrumentation

Bruel & Kjaer type 4321 triaxial accelerometers (1) with Bruel & Kjaer type 2635 charge amplifiers were used to monitor the response on the tail unit. The input force at the point of excitation was measured by the use of a B & K type 8200 force transducer. Data acquisition and processing were done using the Gen-Rad type 2515 Signal Analysis System while Modal Analysis was performed using the SDRC Modal Plus software package [2].

Accelerometer mounting and exciter attachment on the composite structure employing conventional methods presented some problems as direct hole drilling on the structure was not practicable. Use of carpet fixing double-sided adhesive tape ("SYROM") for accelerometer mounting was found to be efficient upto 5 kHz. The exciter quill shaft was attached by means of Methylmethacrylic Glue Type X 60 providing the required tenacity.

2.3 Procedure

The composite Tail Unit was divided into a number of elements and was schematized as shown in figure 2 for purposes of this study. These elements were identified by numbers as shown in figure 3.

2.3.1. Selecting excitation point

The next step was to select a reference point [3] (point of excitation) so that all pure modes of the structure could be excited. This survey for the reference point was conducted by impulsive excitation using a hammer with a steel tip. Three points, 8, 29 and 40 (figure 29) were selected for excitation in the y-direction (lateral direction).

It was noticed that the autospectrum of the force (figure 4) decayed off sharply around 1 kHz and the Transfer Functions at reference points 8, 29 and 40 (figure 5) showed an increasing trend for the modulus indicating the presence of useful information beyond 1 kHz which the impulsive type of excitation could not, perhaps, unfold (to facilitate easy identification, functions have been separated from each other by multiplying them opportunely by a scale factor - ordinate only - in the figure).

2.3.2. Selection of type of excitation

In order to proceed further it was decided at this stage to select the type of excitation for modal study and to do this survey the structure was excited laterally (y-direction) at the reference point 40 in the frequency range 0-1 kHz. The frequency range was divided in two parts i.e. 0-500 Hz and 500-1000 Hz for better resolution. The following three methods of excitation were employed:

- Impact
- Random
- Swept Sine with a duration of 180 seconds for a complete sweep.

The response at the reference point was measured in each case and the Transfer Function was plotted as shown in figs. 6 and 7. On an examination of the response, random excitation was chosen to excite the structure as this gave a better coherence (i.e. signal to noise ratio) and was less time consuming in addition to being much easier to handle.

The structure was then excited laterally at points 8, 11, 29 and 40 (figure 8) in the frequency range 100-2000 Hz as no sensible peaks were observed below 100 Hz. From the response at the four points (c.f. figure 9, 10, 11 and 12) it was observed that the reference point 40 was the most efficient. An extra point of reference, point 11, was chosen to get a better insight.

For excitation of the structure in the vertical direction (z direction) points 8 and 39 were chosen (figure 13). The response at 8 and 39, using random excitation, was plotted as shown in figure 14, from which it could be seen that point 39 was more efficient.

It is to be noted that at point 39 the direction of excitation was at 45° in the X - Z plane. Although this could lead to an incorrect estimation of the amplitude residue the resonance frequencies would still be correct. However, as the amplitude residue is affected by a bias error this can easily be compensated for.

2.3.3. Reciprocity and Linearity checks

Reciprocity checks were performed using points 8 and 40. The responses were plotted as shown in figures 15, 16, 17, 18. The disagreement observed at places (between 400-450 Hz and above 750 Hz) suggested non linearities in the structure.

A linearity check was then performed at point 40 employing a sine dwell technique at three different force levels (5, 10 and 20 N at 657 Hz peak).

The results as plotted in figures 19 and 20 showed perfect agreement at the three force levels. This suggested that the disparity noticed in the reciprocity checks were due to the presence of local modes rather than to non-linearities. In fact, this led us to look only modes, at best, upto 700 Hz.

3. Analysis

3.1 Modal Parameter extraction

The extraction of modal parameters was performed using different techniques in order to obtain the most representative set of data.

In order to estimate the number and the importance of the modes present in the frequency range studied, Indicator Functions [4] based on different sets of functions were calculated.

At the beginning of the analysis all the modal parameters were evaluated by means of the Direct Parameter Estimation technique [5] which is a NDOF frequency domain curve fitting algorithm. This technique manipulates multiple response functions from a single reference point to obtain global least squares estimates of the modal properties. Then parameters were checked by means of time domain estimation technique typically the Complex Exponential technique [6] in order to verify and improve the accuracy of the previous extraction method.

An effort to validate the modal data base was done. This operation permitted to check the parameter and mode shape estimation techniques and helped a review of the parameter tables.

Two mode shapes (465 and 370 Hz), neglected on first approach, were found and calculated, and a review of a critical damping value was performed. Damping factors were changed in some cases upto about 30% of their previous estimation in order to have a better analytical synthesis of the experimental data. A complete list of the Parameter set is shown in Table 1. From this table we see that the resonance frequencies range from 124 Hz to 600 Hz highlights the high stiffness of the carbon fiber material with respect to its low weight.

Besides we note a low damping ratio which is about half the value usually found in aeronautical structures.

3.2 Mode shape extraction

As the parameter set was calculated by means of the Direct Parameter Estimation Technique the same approach was first chosen in mode shape calculation.

All the shapes were also computed by means of single Degree of Freedom Circle Fit technique to avoid the black box effect occurring when using automatic routines.

The final choice of a mode shape was made using the SDOF Circle Fit Technique which allowed a better control on the mode shape extraction. In fig. 25 are shown two mode shapes at 124 and 143 Hz as calculated by Direct residue extraction (left) and by SDOF Circle Fit Techniques (right). Modal assurance criterion was in this case 0.24 indicating a not very good shape correlation. The two sets of data were compared by means of Modal Assurance Criterion Technique [4]. Good correlation was not always found and because of this new evaluation of some mode shapes by means of SDOF Circle Fit technique [7] was performed.

In some cases differences did not disappear.

This could be due to some complex modes that could not be well calculated by means of the SDOF Circle Fit Technique.

3.3 Mode shape descriptions

In the following a brief description of main mode shapes is presented. Due to the high number of modes it is sometimes difficult to give a simple description of a mode.

Better interpretation can be obtained by an animation on a computer video.

Shape	Frequency (Hz)	Description
1	124.143	Vertical fin first lateral bending with rigid motion of the tail cone.
2	148.611	Local mode of fin tip overlapped with longitudinal motion of vertical fin.
3	162.358	Vertical fin first longitudinal bending.
4	212.105	Vertical fin first torsional.
5	236.245	Vertical fin second lateral bending.
6	248.175	Vertical fin torsion.
7	289.023	Vertical fin second lateral bending.
8	297.620	Vertical fin torsion and bending.
9	313.455	Vertical fin third lateral bending.
10	343.430	Tail cone first lateral bending.
12	379.419	Tail cone second lateral bending.

14	387.748	Tail cone first lateral bending
19	506.143	Tail cone first torsional mode.

For Modes 15th up to 18th a precise description is not possible, with this geometry, because of "shape aliasing". Modes from 20th to 23rd can be defined as upper Global modes.

Figures 27 to 49 show how the specimen moves at the various frequencies. We note that the upper fin and the tail cone behave in a quite different manner because of the different form and stiffness. The tail cone, in fact, has its first resonance frequency at 343 Hz which is about three times the vertical fin first frequency.

4. Conclusion

This paper has analysed the procedure and the difficulties encountered in conducting an experimental dynamic analysis of a composite structure.

In particular the analysis for the BHI01 model composite Tail Unit has evidenced:

- Feasibility of random excitation.
- Low attenuation of modes.
- Relatively high resonant frequency.
- Distinct mode separation between upper fin and Tail Cone.

A natural follow up of this effort is to analyze the full scale tail unit and compare the two sets of results in order to verify the feasibility of the model in the search and determination of natural frequencies in a composite structure.

Bibliography

- [1] Piezoelectric Accelerometers and Vibration amplifiers - Theory and Application Handbook - Mark Serridge BSc and Torben R. Licht, MSc. BRUEL & KJARR October 1986.
- [2] SDRC - Reference Manual for Modal Plus 9.0 SDRC CAB International.
- [3] Modal Testing: Theory and practice - D.J. Ewins Bruel & Kjaer - 1986.
- [4] SDRC - User Manual for Modal Analysis SDRC CAB International.
- [5] Advanced matrix methods for experimental modal analysis - A multi matrix method for direct parameter extraction - Leuridan, J. - Kundrat, J. 1st International modal analysis conference.
- [6] Solving least squares problems-Lawson, C.L. - Hanson, R.J. - Prentice hall 1974.
- [7] Theoretical background of curve-fitting methods used by Modal Analysis-"Modal Analysis Seminar" Leuven 1979.

Modal Parameters		
Label	Freq	Damping
1	124.143	0.01432
2	148.611	0.00871
3	162.358	0.00751
4	212.105	0.01732
5	236.245	0.01346
6	248.175	0.00832
7	289.023	0.01210
8	297.520	0.00670
9	313.455	0.00483
10	343.430	0.00617
11	370.445	0.01837
12	379.419	0.00430
13	387.748	0.00167
14	394.937	0.01218
15	436.467	0.00812
16	453.345	0.00847
17	465.279	0.01323
18	498.696	0.00555
19	506.143	0.01379
20	520.482	0.01133
21	524.852	0.02202
22	529.995	0.01249
23	601.493	0.00976

TAB 1

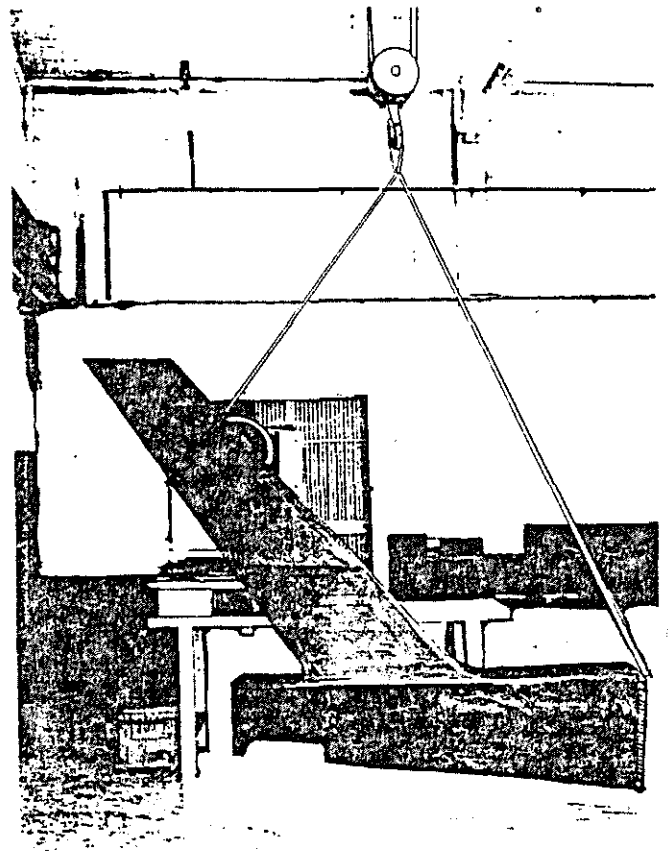


Fig. 1 Model Tail Unit

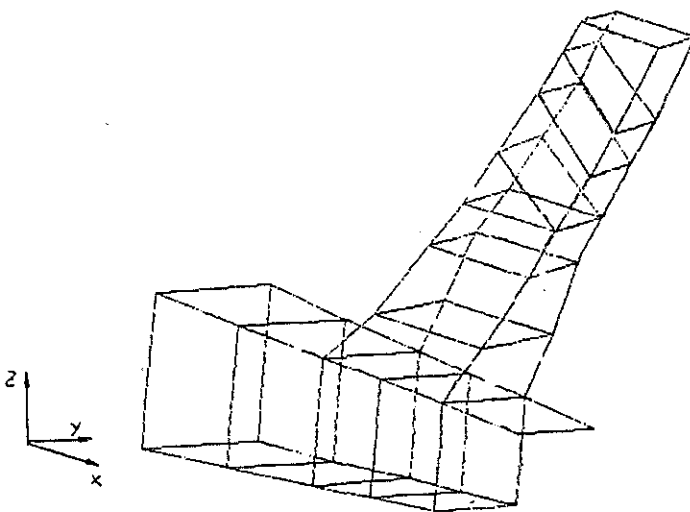


Fig. 2 Tail Unit Schematization

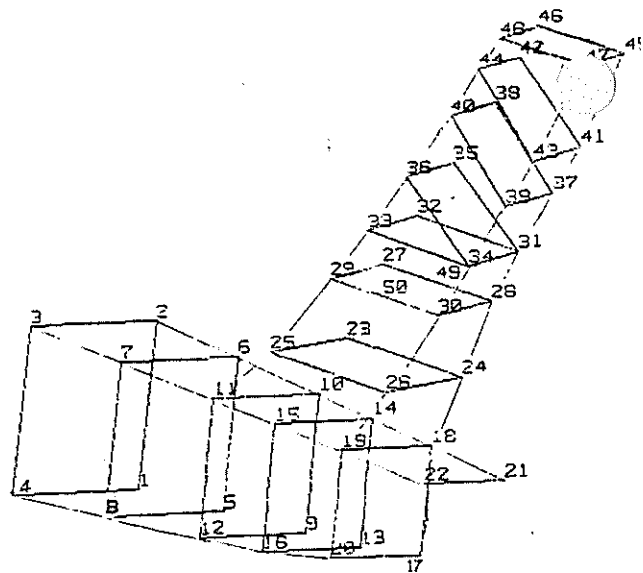


Fig. 3 Tail Unit location numbers

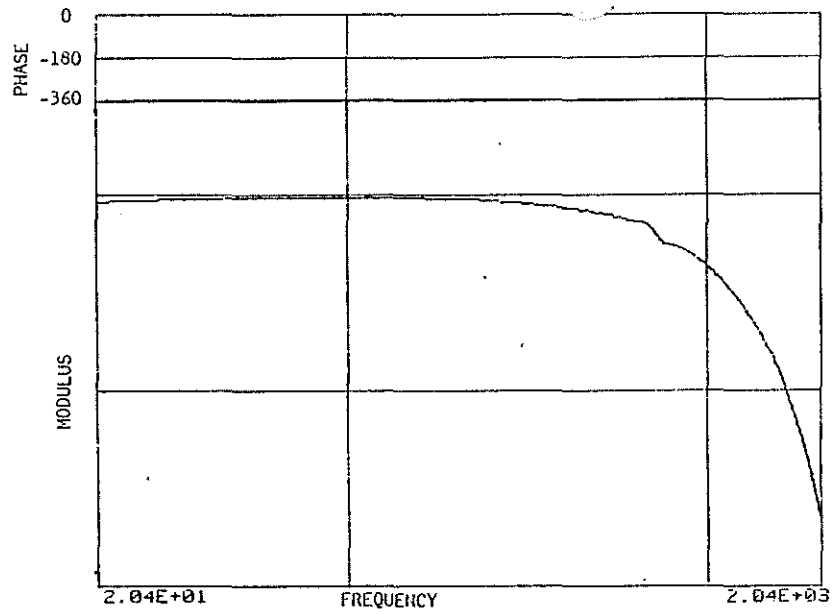


Fig. 4 Force autospectrum - Hammer with steel tip

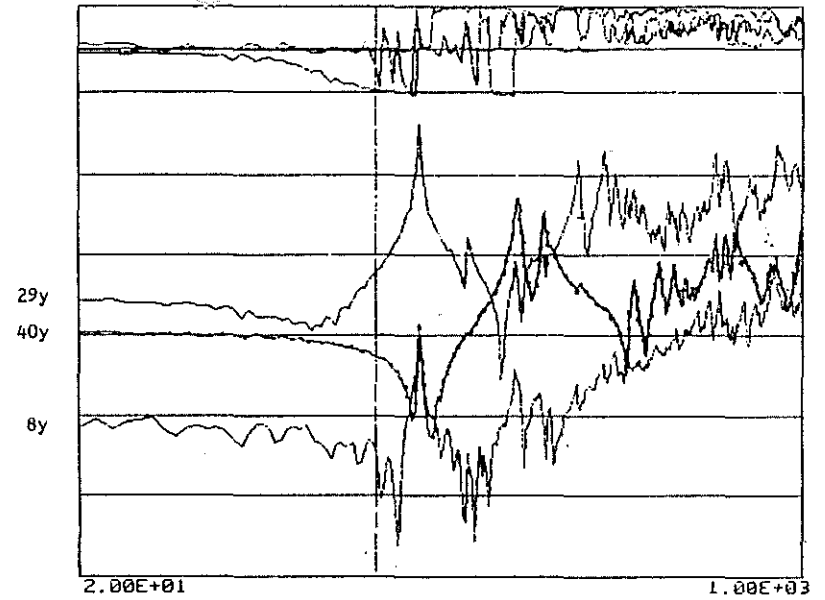


Fig. 5 Transfer Function at reference points 8, 29 and 40

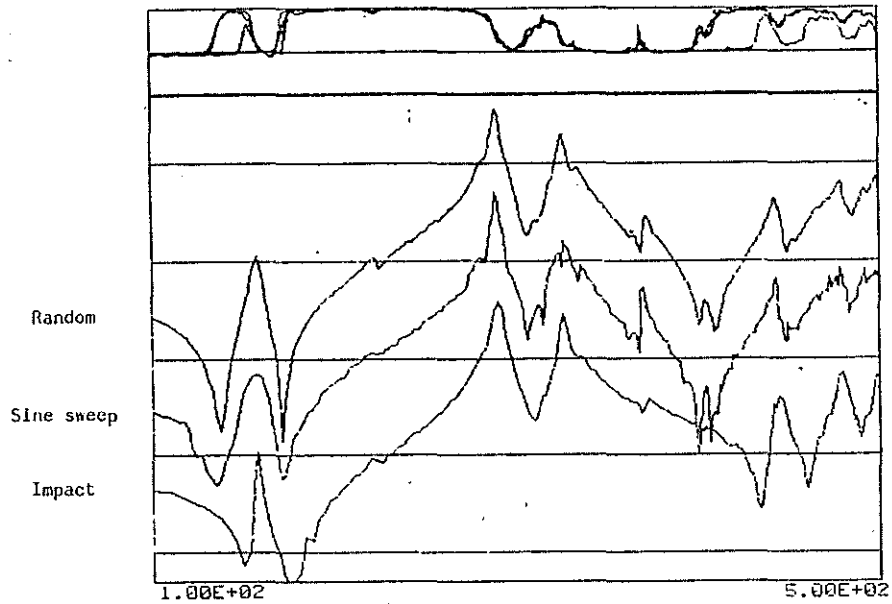


Fig. 6 Transfer Function 100 - 500 Hz with different kinds of excitation at point 40y

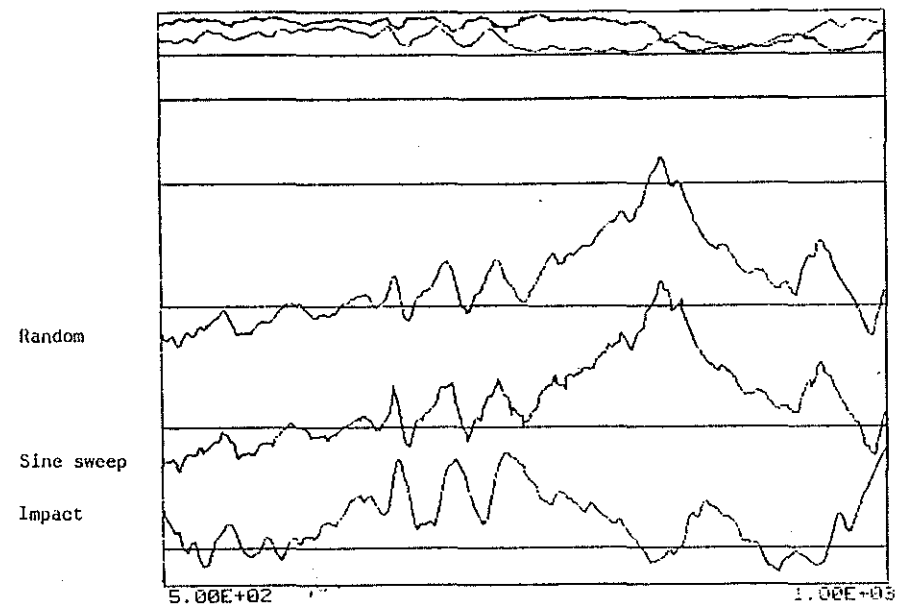


Fig. 7 Transfer Functions 500 - 1000 Hz with different kinds of excitation at point 40y

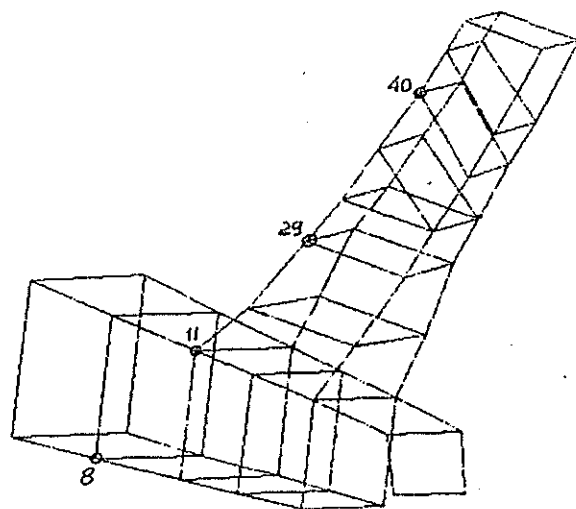


Fig. 8 Reference points

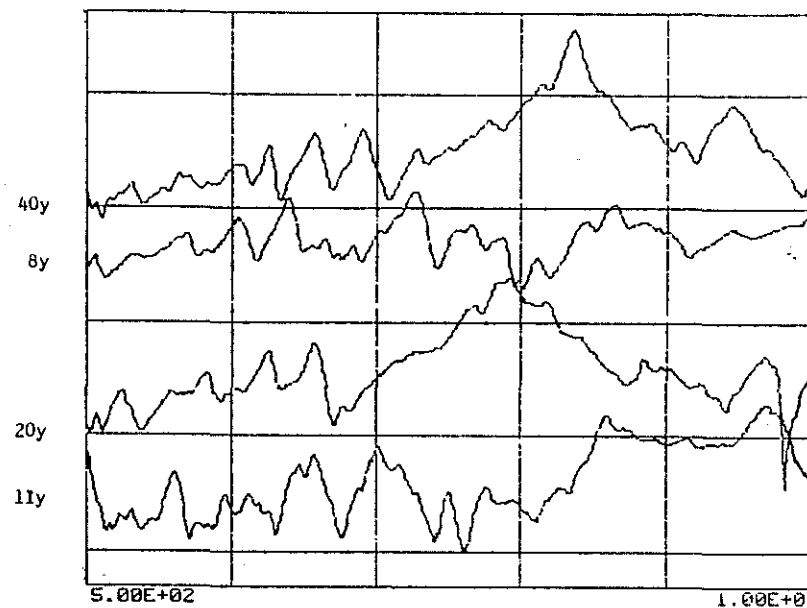


Fig. 10 Reference search - Transfer Functions at different points - Frequency range 500 - 1000 Hz

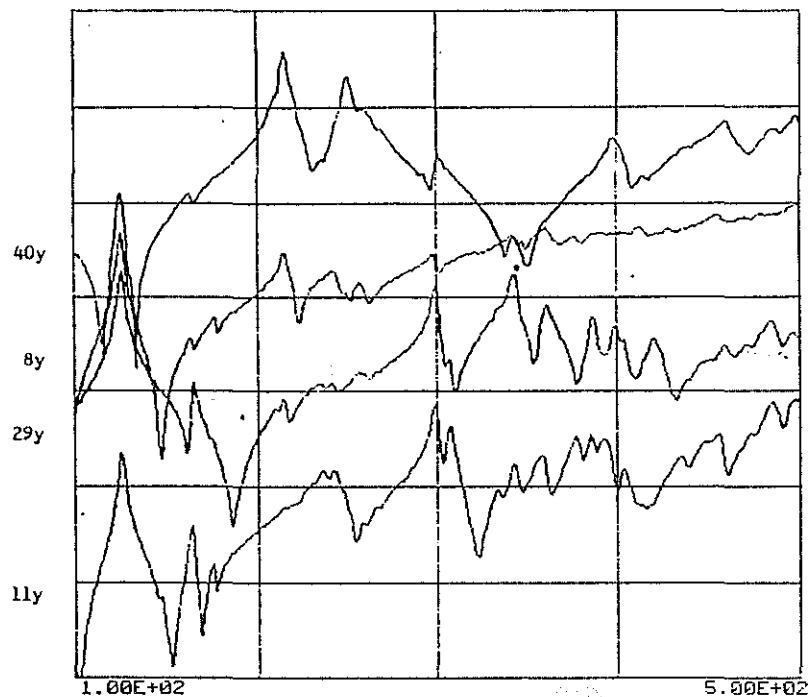


Fig. 9 Reference search - Transfer Function at different points - Frequency

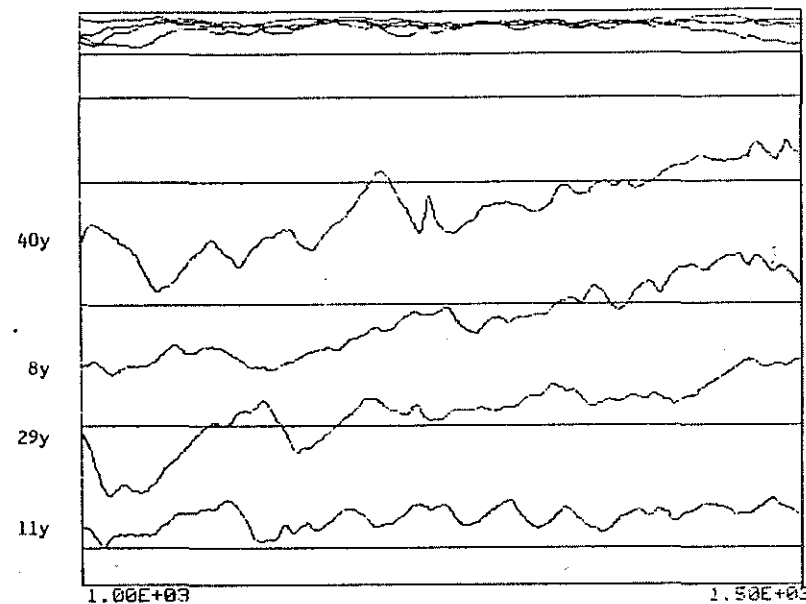


Fig. Reference search - Transfer functions at different points - Frequency range 1000 - 1500 Hz

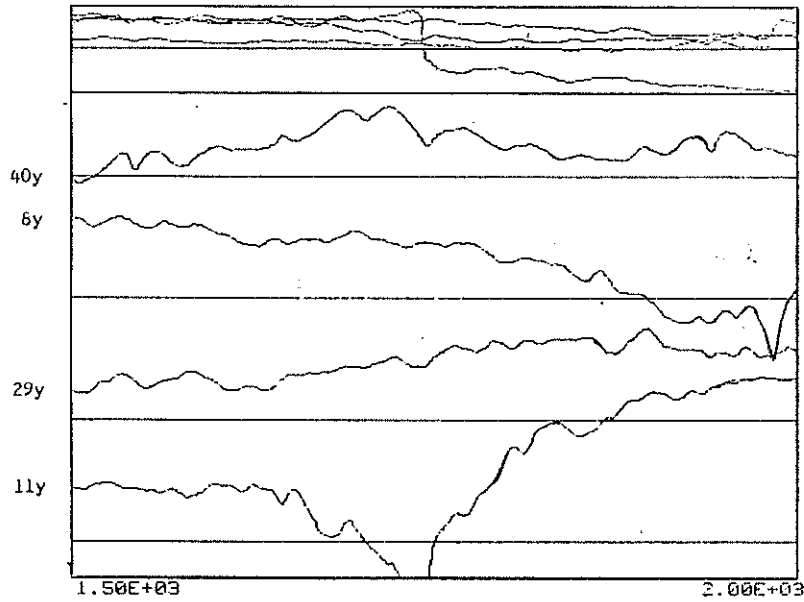


Fig. 12 Reference search - Transfer Functions at different points - Frequency range 1500 - 2000 Hz

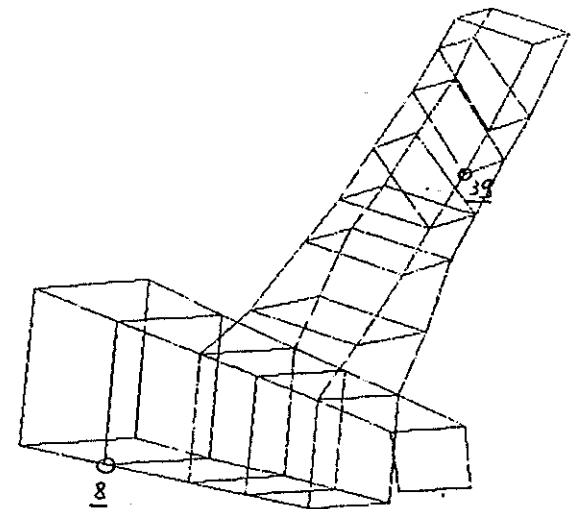


Fig. 13 Reference points

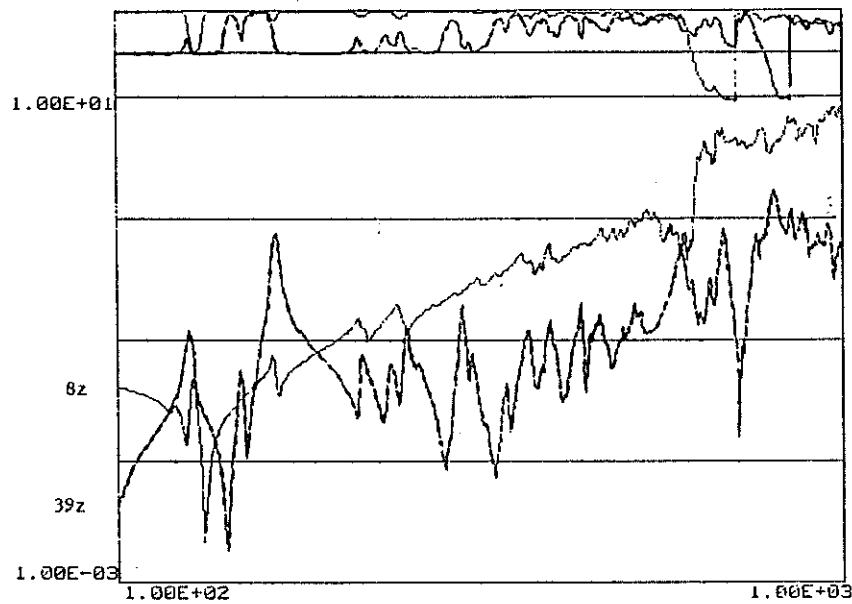


Fig. 14 Reference response functions

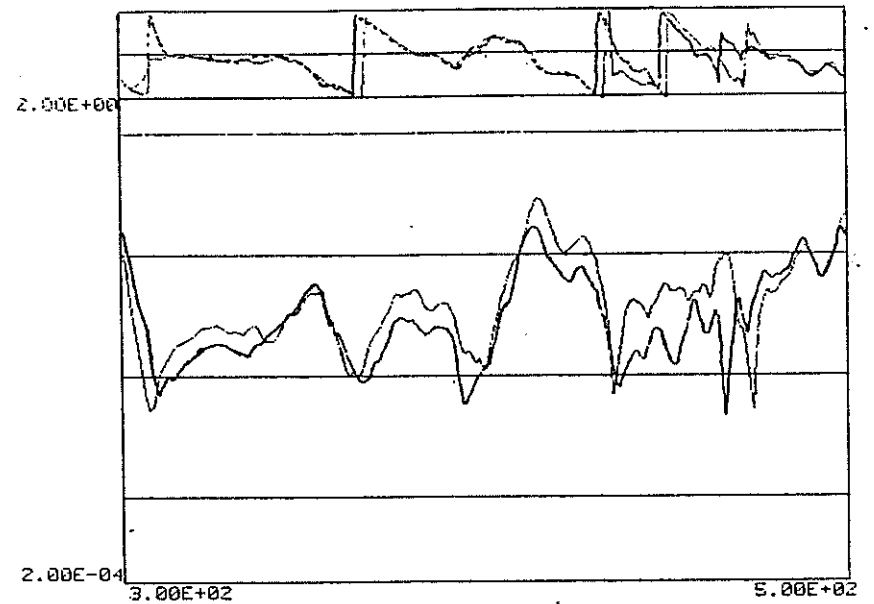


Fig. 15 Reciprocity checks 300-500 Hz — 40Y+ 39Y — 8Y 40Y

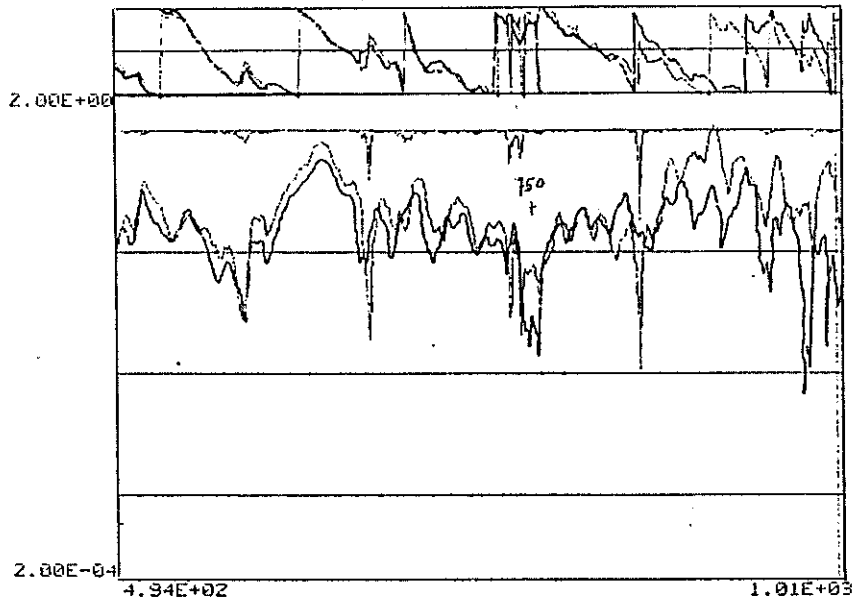


Fig. 16 Reciprocity checks 500 - 1000 Hz — 40Y+ 8Y+
— 8Y 40Y

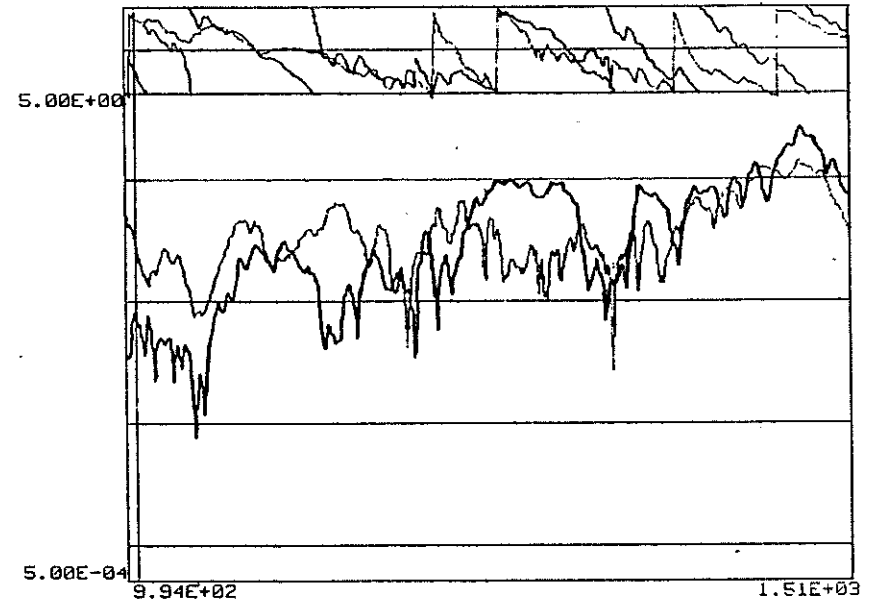


Fig. 17 Reciprocity checks 1000 - 1500 Hz — 40Y+ 6Y+
— 8Y 40Y

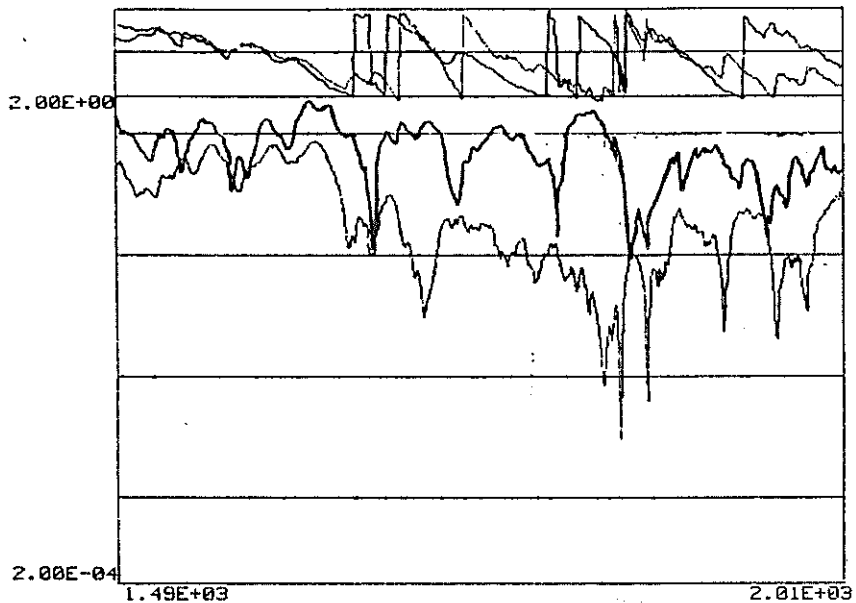


Fig. 16 Reciprocity checks 1500 - 2000 Hz — 40Y+ 8Y+
— 8Y 40Y

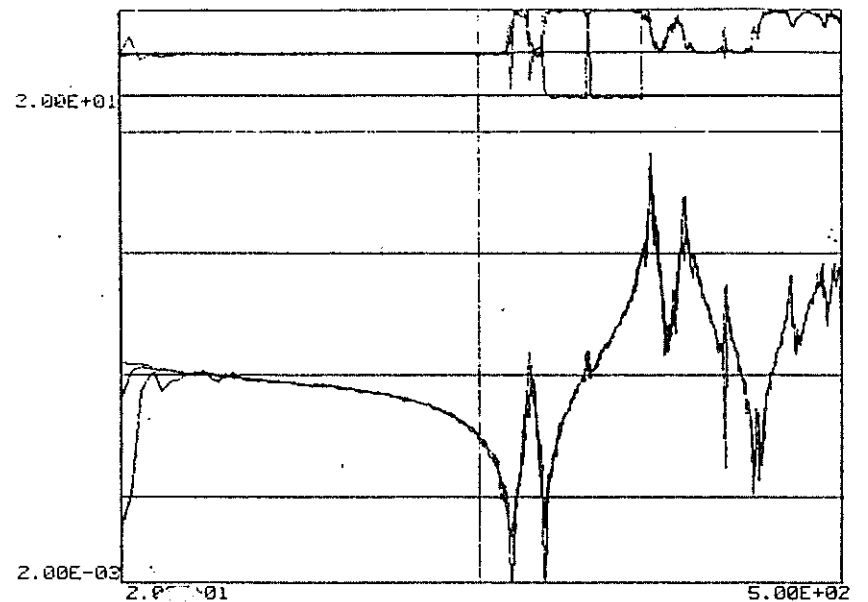


Fig. 17 Linearity checks 200 - 500 Hz

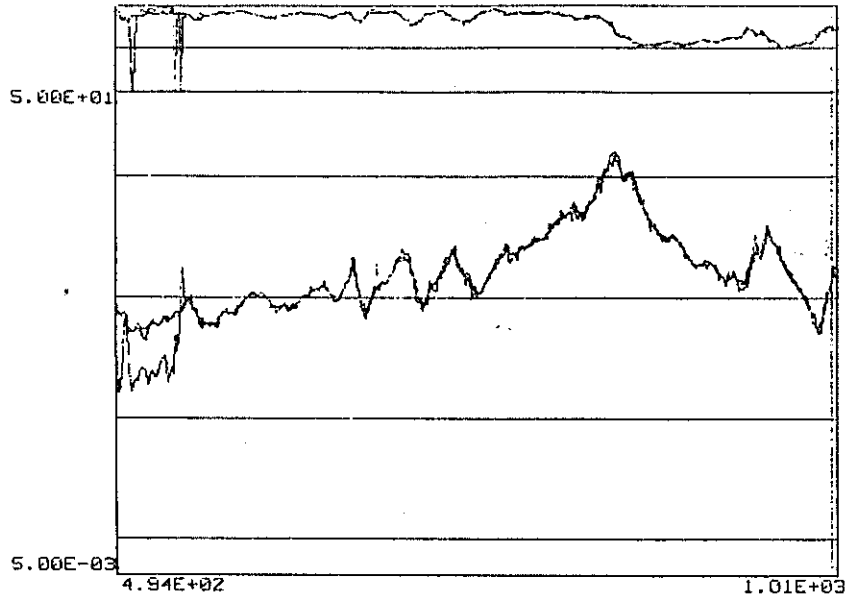


Fig. 20 Linearity checks 500 - 1000 Hz

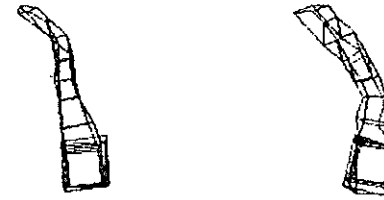


Fig. 21 Freq. 124.143 Hz
Direct Residual extraction (left)
SDOF Circle Fit Technique (Right)

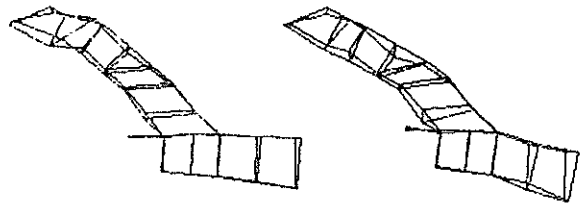


Fig. 22 Freq. 162.358 Hz
Direct Residual extraction (left)
SDOF Circle Fit Technique (Right)

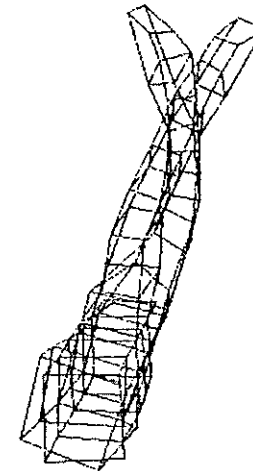


Fig. 23 Frequency 124.143 Hz

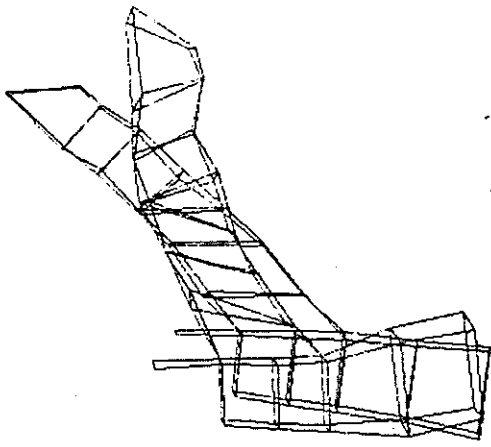


Fig. 24 Frequency 148.611 Hz

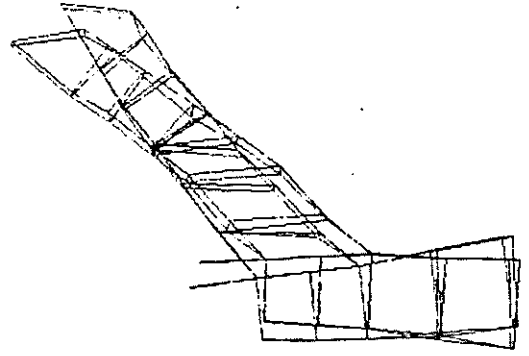


Fig. 25 Frequency 162.358 Hz

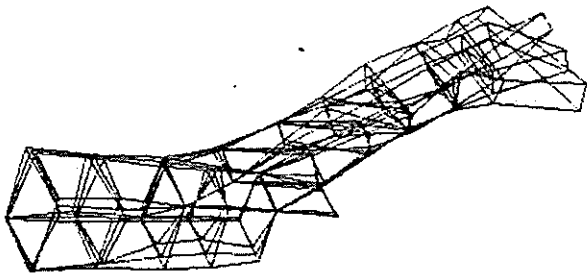


Fig. 26 Frequency 212.105 Hz

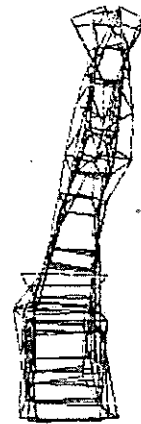


Fig. 27 Frequency 236.245 Hz



Fig. 28 Frequency 248.175 Hz



Fig. 29 Frequency 289.023 Hz

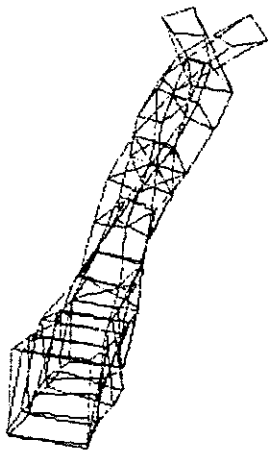


Fig. 30 Frequency 297.620 Hz

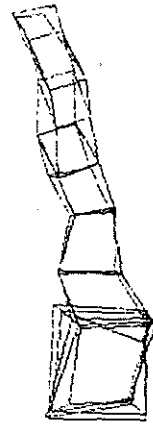


Fig. 31 Frequency 313.455 Hz

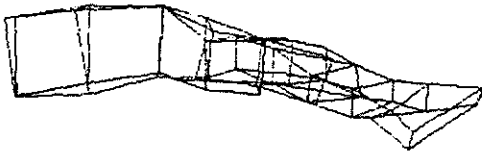


Fig. 32 Frequency 343.430 Hz



Fig. 33 Frequency 370.445 Hz

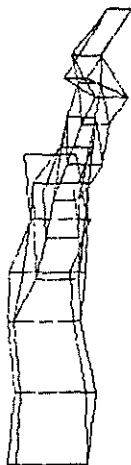


Fig. 34 Frequency 379.419 Hz

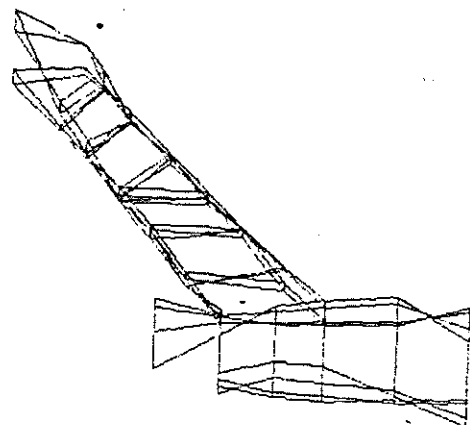


Fig. 35 Frequency 387.748 Hz

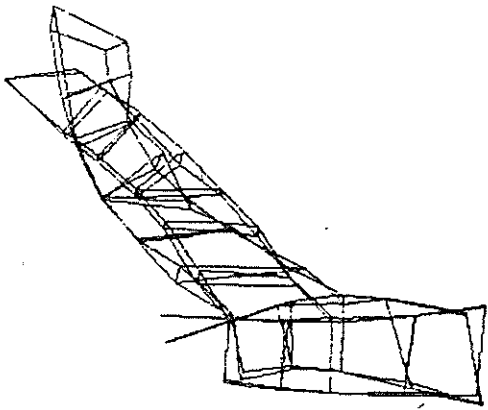


Fig. 36 Frequency 394.937 Hz

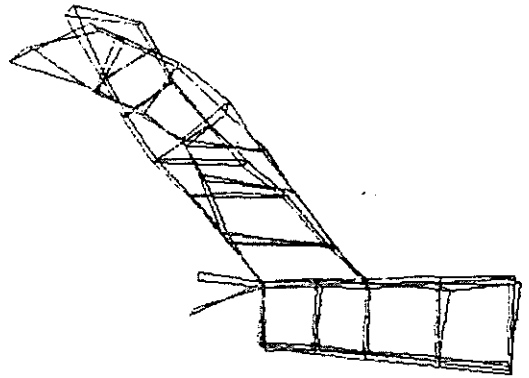


Fig. 37 Frequency 436.467 Hz

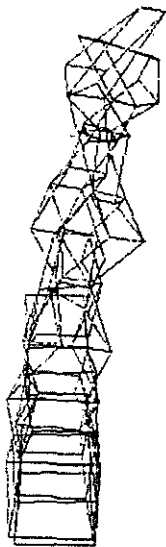


Fig. 38 Frequency 453.345 Hz

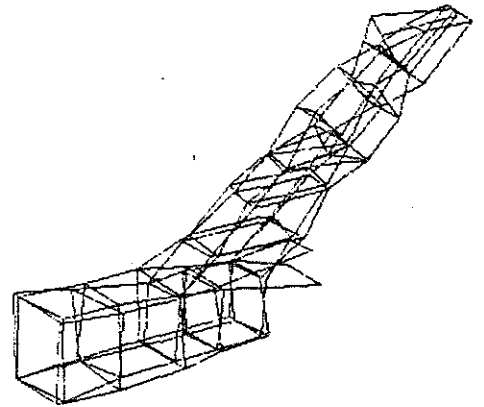


Fig. 39 Frequency 465.278 Hz

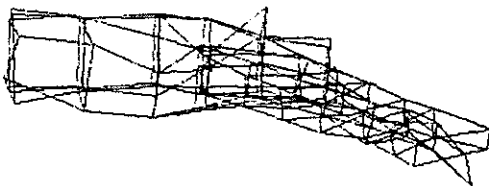


Fig. 40 Frequency 498.696 Hz

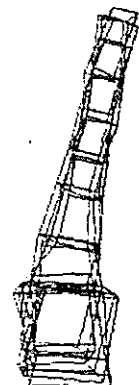


Fig. 41 Frequency 506.143 Hz

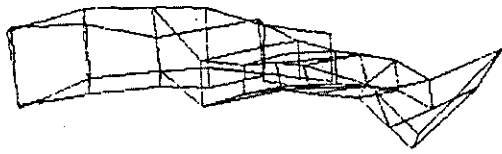


Fig. 42 Frequency 520.482 Hz

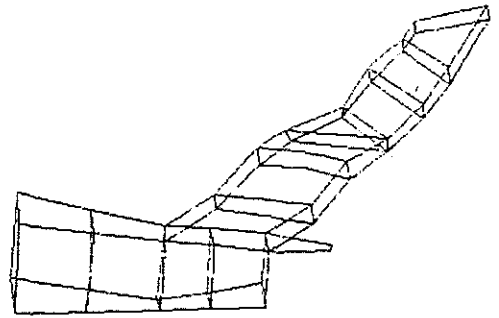


Fig. 43 Frequency 524.852 Hz

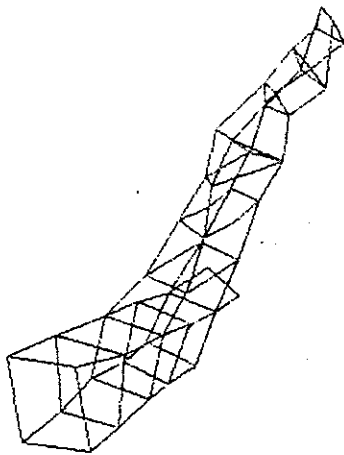


Fig. 44 Frequency 529.995 Hz

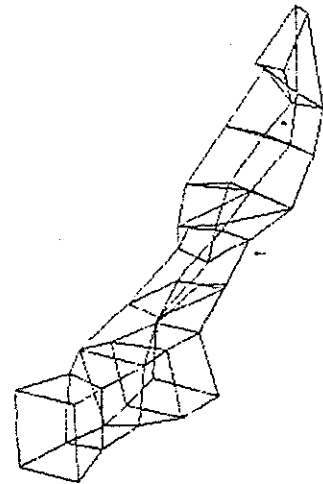


Fig. 45 Frequency 601.493 Hz